Polymer Journal (2020) 52:1375–1385
https://doi.org/10.1038/s41428-020-0387-9

ORIGINAL ARTICLE

Photo-responsive polymer micelles from *o*-nitrobenzyl ester-based amphiphilic block copolymers synthesized by mechanochemical solid-state copolymerization

Naoki Doi[1] · Yukinori Yamauchi[2] · Ryo Ikegami[1] · Masayuki Kuzuya[1,3] · Yasushi Sasai[4] · Shin-ichi Kondo[1]

Received: 16 April 2020 / Revised: 19 June 2020 / Accepted: 24 June 2020 / Published online: 31 July 2020

Abstract

Polymer micelles with a tunable drug release would be suitable for the concept of drug delivery system. We constructed photo-responsive polymer micelles from amphiphilic block copolymers. The polymer micelles were synthesized by mechanochemical solid-state copolymerization of poly[*N*-(2-hydroxypropyl)methacrylamide] (PHPMA) and 4,5-dimethoxy-2-nitrobenzyl methacrylate as a photosensitive moiety. The above mechanochemical solid-state copolymerization was performed by vibratory-ball milling at 30 Hz in a nitrogen atmosphere with the use of an agate vessel and an agate ball to yield amphiphilic block copolymers (PHPMA-*b*-PDNMA). Spherical polymer micelles were formed by the self-assembly of PHPMA-*b*-PDNMA. The diameter of the PHPMA-*b*-PDNMA micelles was in the range of 130-200 nm. The PHPMA-*b*-PDNMA micelles loaded with the antitumor drug 5-fluorouracil (5-FU) showed photo irradiation induced time-dependent release of 5-FU with an associated decrease of micellar size. The drug release profile of the PHPMA-*b*-PDNMA micelles followed a clear sigmoid curve. Our approach provides a controlled drug release system through the use of photo-responsive polymer micelles, accompanied by the gradual decrease of micellar size.

Introduction

Polymer micelles, which are formed by the self-assembly of amphiphilic block copolymers, have extensively attracted much attention in drug delivery system, especially as drug carriers for antitumor drugs [1–3]. Polymer micelles incorporating antitumor drugs could exhibit favorable therapeutic advantages: prolonged circulation time compared to the drug administration without them, avoiding the reticuloendothelial system and renal clearance, passive targeting into tumor tissues by the enhanced permeability and retention effect [4–8].

In past decades, stimuli-responsive polymer micelles that could respond to temperature [9–12], light [13–17], ultrasound [18–21], and pH [22–27] have emerged as effective drug carriers, improving the performance of a controlled drug release. Among the various types of external stimuli, photo irradiation is of particular interest because the on-off switching of drug release from photo-responsive polymer micelles can be expected. Photo-responsive polymer micelles, which can be disrupted by photo irradiation, are classified into two types. Cis-trans isomerization groups (e.g., azobenzene and stilbene) and photoinduced shifting groups (e.g., spiropyran, dithienylethene, and diazonaphthoquinone) that shift from hydrophobic to hydrophilic are used as reversible photo-responsive moieties due to their structural changes upon photo irradiation. In the case of an irreversible response, photocleavable groups (e.g., pyrene, *o*-nitrobenzyl, and coumarin) can be introduced to the main chain and/or pendant groups of the block copolymers for disassembly of the polymer micelles. Among the various photocleavable groups, *o*-nitrobenzyl esters would especially

Supplementary information The online version of this article (https://doi.org/10.1038/s41428-020-0387-9) contains supplementary material, which is available to authorized users.

✉ Shin-ichi Kondo
skondo@gifu-pu.ac.jp

[1] Laboratory of Pharmaceutical Physical Chemistry, Gifu Pharmaceutical University, 1-25-4, Daigaku-nishi, Gifu 501-1196, Japan

[2] Department of Pharmaceutical Physical Chemistry, College of Pharmaceutical Sciences, Matsuyama University, 4-2 Bunkyo-cho, Matsuyama, Ehime 790-8578, Japan

[3] Department of Health and Welfare, Faculty of Human Welfare, Chubu Gakuin University, 2-1 Kirigaoka, Seki, Gifu 501-3993, Japan

[4] Faculty of Pharmacy, Gifu University of Medical Science, 4-3-3 Nijigaoka, Kani, Gifu 509-0293, Japan

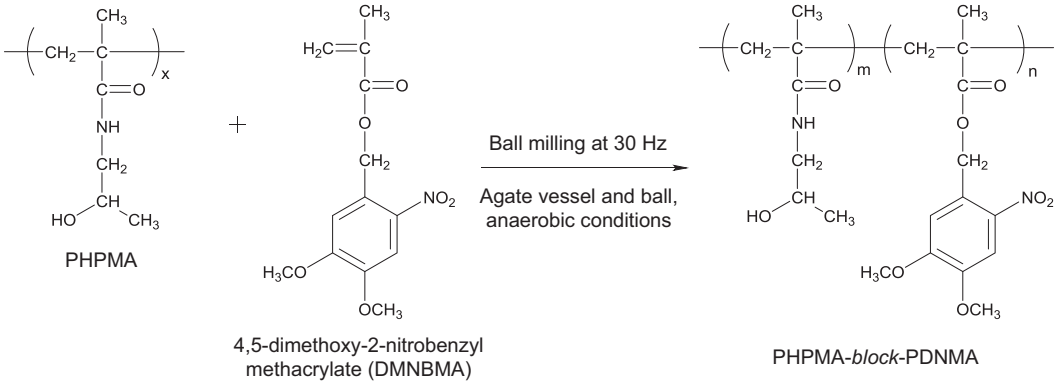

Fig. 1 Schematic representation showing the mechanochemical solid-state copolymerization of PHPMA and DMNBMA

be useful for forming a compact micellar core due to steric advantages. Zhao et al. extensively reviewed the photochemical reaction mechanisms of *o*-nitrobenzyl ester groups [28]. *o*-Nitrobenzyl ester groups produced a corresponding *o*-nitrosobenzaldehyde under UV irradiation, simultaneously releasing a free carboxylic acid compound in the presence of H_2O. Therefore, polymer micelles possessing *o*-nitrobenzyl esters as side chains in their hydrophobic segments can be decomposed by a conformational change because the hydrophobic segments change to being hydrophilic by UV-light exposure. Zhao's group has also explored photo-responsive polymer micelles based on poly(ethylene oxide)-*b*-poly (nitrobenzyl methacrylate) [29] and poly(ethylene oxide)-*b*-poly(ethoxytri(ethyleneglycol)acrylate-*co*-nitrobenzylacrylate) [30]. However, the drug release profile and micellar dissociation kinetics of photo-responsive polymer micelles have not yet been studied; thus, their elucidation should be useful for designing various pharmacotherapeutics with the photo-responsive polymer micelles.

Amphiphilic block copolymers with narrow heterogeneity and well-defined structures have been successfully synthesized by living radical polymerization (e.g., atom transfer radical polymerization (ATRP) and reversible addition fragmentation chain transfer (RAFT) polymerization). However, ATRP and RAFT polymerization generally require the addition of metal catalysts and an RAFT chain transfer agent, respectively, and the removal of these additions after polymerization can be expensive and time-consuming [31–33].

We have reported that mechanoradicals generated by polymer main-chain scission via ball milling of solid polymers play an important role as macro-initiators in the presence of solid vinyl monomers; hence, the solid-state polymerization of solid vinyl monomers proceeds to produce block copolymers [34–44]. Mechanochemical solid-state copolymerization does not require the addition of catalysts or solvents. Recently, we demonstrated that polymer micelles from amphiphilic block copolymers with pendant pyridyl groups, which were synthesized via mechanochemical solid-state copolymerization, were stable in pH 7.4, while dissociating into its block copolymers in pH 5.4 [24]. Furthermore, when loaded with antitumor drugs, these pH-responsive polymer micelles indicated cytotoxicity in vitro [25].

In this work, we designed and synthesized a novel amphiphilic block copolymer composed of poly[*N*-(2-hydroxypropyl)methacrylamide] (PHPMA) and poly(4,5-dimethoxy-2-nitrobenzyl methacrylate) (PDNMA) having photo-responsive *o*-nitrobenzyl ester groups via mechanochemical solid-state copolymerization (Fig. 1). PHPMA possesses high water solubility, non-immunogenicity, and biocompatibility, so we used it as the hydrophilic chains of the polymer micelles [45–48]. As the maximum absorption wavelength ($\lambda = 400$ nm) of PDNMA is longer than that of 2-nitrobenzyl-methacrylate (or acrylate), it was hypothesized that PDNMA might decompose in nearly visible light. Thus, we selected PDNMA as a photo-responsive moiety. As shown in Fig. 2, photo-responsive PHPMA-*b*-PDNMA micelles encapsulating antitumor drugs, 5-fluorouracil (5-FU), in the micellar core were prepared by a dialysis method, and the physicochemical properties (e.g., drug loading content (DLC), drug loading efficiency (DLE), stability in aqueous solution, and micellar size and shape) were determined by dynamic light scattering (DLS), transmission electron microscopy (TEM) imaging, and UV-Vis spectroscopy. Our ultimate goal regarding the photo-responsive polymer micelles was to reveal the drug release profile and decrease in micellar size via photo irradiation. In addition, we examined the behavior of the micellar core by photolysis of the hydrophobic regions.

Materials and methods/experimental procedures

Materials for the synthesis of the monomers and polymers

(±)-1-Amino-2-propanol (Fujifilm Wako Pure Chemical Corp., purity ≥ 99.0%) was used as received. Prior to use, triethylamine (TEA) (Kishida Chemical Co., Ltd,

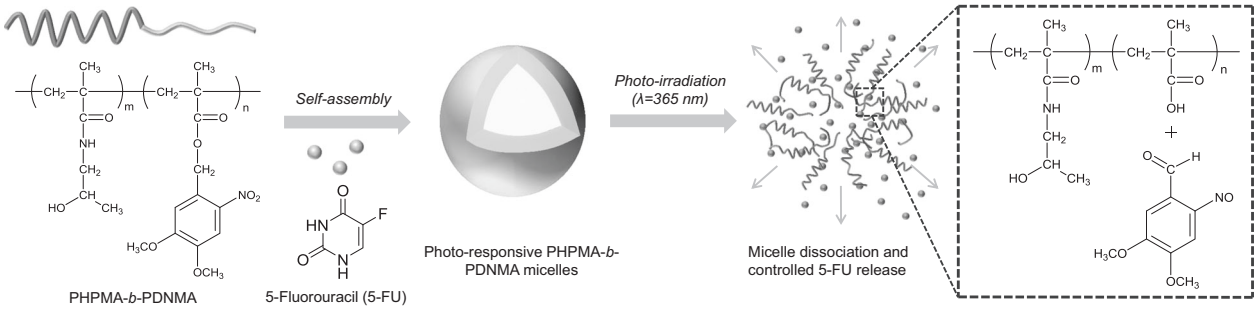

Fig. 2 Schematic illustration showing the preparation and disassembly of photo-responsive 5-FU-loaded PHPMA-*b*-PDNMA micelles and the corresponding 5-FU release due to micellar dissociation via photo irradiation

purity ≥ 99.0%) was distilled. Dichloromethane (DCM) (Kanto Chemical Co., Inc, purity ≥ 90.0%) was dried over CaH_2 (Nacalai Tesque Inc, purity ≥ 90.0%) and distilled. Methacryloylchloride (Tokyo Chemical Industry Co., Ltd, purity ≥ 99.0%) was purified by distillation under reduced pressure in a nitrogen atmosphere. *N,N*-Dimethylformamide (DMF) (Kanto Chemical Co., Inc, purity ≥ 99.5%) was distilled under reduced pressure and stored over 4 Å molecular sieves. 4,5-Dimethoxy-2-nitrobenzyl alcohol (Fujifilm Wako Pure Chemical Corp., purity ≥ 95.0%) was used without purification. Sodium sulfate (Nacalai Tesque Inc, purity ≥ 98.5%) and sodium phosphotungstate (Nacalai Tesque Inc, purity ≥ 98.0%) were used without further treatment. 2′,2′-Azobis[2-(2-imidazolin-2-yl)-propane]dihydrochloride (Fujifilm Wako Pure Chemical Corp., purity ≥ 97.0%) was used as received without further purification. 5-FU (Tokyo Chemical Industry Co., Ltd, purity ≥ 99.0%) was used directly. Spectra/Por® 3 dialysis membrane standard RC tubing (molecular weight cut-off (MWCO), 3500) was purchased from Spectrum Laboratories, Inc. Milli-Q water (Millipore, 18.2 MΩ cm at 25 °C) was used in all experiments. Other reagents were used as received.

Characterization

^{1}H NMR spectra were recorded on a JEOL ECA500 FT-NMR spectrometer in dimethyl sulfoxide-d_6 (DMSO-d_6) containing tetramethylsilane (0.1%(w/v)) as an internal standard. The samples fractured in a nitrogen atmosphere were exposed to air to quench the radicals, and then the ^{1}H NMR spectra were measured. The ratio of polymer conversion was estimated based on the rate of decrease of 4,5-dimethoxy-2-nitrobenzyl methacrylate (DMNBMA) olefinic proton peaks compared with the constant signal of the added maleic acid (0.8%(w/v)).

The molecular weight of each resulting polymer was measured by gel permeation chromatography (GPC) in DMF containing 100 mM LiBr at 40 °C (flow rate: 0.7 mL min^{-1}). Three kinds of styrene divinylbenzene copolymer gel columns (Shodex KD-G 4A: particle size = 8 μm; 4.6 i.d. ×10 mm, Shodex KD-802: exclusion limit = 7000; particle size = 6 μm; pore size: 150 Å; 8.0 i.d. ×300 mm, and Shodex KD-80M: exclusion limit = 4.0×10^8; particle size = 10 μm; pore size: 10,000 Å; 8.0 i.d. ×300 mm) were connected to a PU 880 HPLC pump (GL Sciences Inc) equipped with an RID-6A refractive index detector (Shimadzu Co., Ltd), a model 554 LC column oven (GL Sciences Inc), and a data analyzer (Runtime Instruments Chromato-PRO, Runtime Instruments Ltd). The system was calibrated with polystyrene (PS) standards (Polymer Laboratories: Peak top of molecular weight (M_p) = 4,490, 9,920, 30,300, 60,450, 170,800, 523,000, and 1,186,000 g mol^{-1}).

The absorption spectra were measured with a UV-Vis spectrophotometer (UV-3600, Shimadzu, Japan). The FT-IR spectra were recorded in the range of 4000-650 cm^{-1} on a Frontier system (PerkinElmer, UK) equipped with an attenuated total reflection accessory. The mass spectra were measured on a JMS-T100TD (AccuTOF-TLC) spectrometer (JEOL Ltd, Tokyo, Japan) equipped with an electrospray ionization source in the positive ion mode with the following parameters: scan range, *m/z* 100-1000; drying chamber temperature, 250 °C; orifice1 temperature, 80 °C; orifice1 voltage, 10 V; orifice2 voltage, 5 V; ring lens voltage, 80 V; peak voltage, 2000 V; detector voltage, 2000 V; and nitrogen gas flow rates, 0.7 L min^{-1} (nebulizing gas) and 2.0 L min^{-1} (drying gas). Elemental analyses were performed on a J-Science Micro Corder JM11 with a JMA112 auto sampler.

Synthesis of monomers and block copolymers

Synthesis of *N*-(2-hydroxypropyl)methacrylamide (HPMA)

(±)-1-Amino-2-propanol (1.48 g, 19.8 mmol) and TEA (2.0 g, 19.8 mmol) were dissolved in 100 mL DCM in a nitrogen atmosphere. The solution was cooled at 0 °C, and then methacryloylchloride (2.07 g, 19.8 mmol) was added dropwise to the cooled solution over 30 min. The reaction mixture was stirred at room temperature, and the reaction progress was monitored by thin layer chromatography. After stirring for

12 h, the reaction mixture was filtered, and then the filtrate was evaporated under reduced pressure. The resulting residue was purified by silica gel column chromatography (DCM: MeOH = 9:1) to give HPMA (white solid, 1.86 g, 66% yield). The product was subsequently analyzed by Fourier transform infrared spectrometer (FT-IR, PerkinElmer, Frontier) and ^{1}H NMR (JEOL ECA500 FT-NMR).

^{1}H NMR [500 MHz, DMSO-d_6, $\delta = 0$ ppm (TMS)]: 7.81 (s, 1H, –NH–), 5.65 (s, 1H; –C = CH_2), 5.31 (s, 1H, –C = CH_2), 4.68 (br, 1H; –OH), 3.68 (m, 1H; –CH–), 3.05 (m, 2H, –CH_2–), 1.85 (s, 3H; = C–CH_3), 1.04 (d, 3H; –CH–CH_3); IR (ATR): $\nu = 3300$ (s), 3263 (s), 2974 (m), 1653 (s), 1614 (s), 1546 cm^{-1} (s); HRMS (ESI) *m/z*: $[M + Na]^+$ calcd. for $C_7H_{13}NO_2Na$, 166.0838; found, 166.0841. Anal. calcd. for $C_7H_{13}NO_2$: C 58.72, H 9.15, N 9.78; found: C 58.61, H 9.29, N 9.59.

Synthesis of 4,5-dimethoxy-2-nitrobenzyl methacrylate (DMNBMA)

4,5-Dimethoxy-2-nitrobenzyl alcohol (533 mg, 2.5 mmol) and TEA (405 mg, 2.5 mmol) were dissolved in 100 mL DCM in a nitrogen atmosphere. The solution was cooled at 0 °C, and then methacryloylchloride (261 mg, 2.5 mmol) was added dropwise to the cooled solution over 30 min. The reaction mixture was stirred at room temperature, and the reaction progress was monitored by thin layer chromatography. After stirring for 12 h, the reaction mixture was filtered, and then the filtrate was extracted with H_2O (50 mL) and DCM (50 mL × 2). The combined organic phase was dried over Na_2SO_4 and filtered, and DCM was removed under reduced pressure. The resulting residue was purified by silica gel column chromatography (n-hexane:ethyl acetate = 3:2) to give DMNBMA (dark yellow solid, 480 mg, 68% yield). The product was subsequently analyzed by FT-IR (PerkinElmer, Frontier), UV-Vis spectroscopy (UV-Vis, SHIMADZU, UV-3600) and ^{1}H NMR (JEOL ECA500 FT-NMR).

^{1}H NMR [500 MHz, DMSO-d_6, $\delta = 0$ ppm (TMS)]: 7.73 (s, 1H; Ar-H), 7.26 (s, 1H; Ar-H), 6.11 (s, 1H; –C = CH_2), 5.76 (s, 1H, –C = CH_2), 5.48 (s, 2H; Ph–CH_2–), 3.95 (s, 3H; –O–CH_3), 3.88 (s, 3H, –O–CH_3), 1.92 (s, 3H; = C–CH_3); IR (ATR): $\nu = 2972$ (w), 2930 (w), 1708 (m), 1580 (m), 1522 cm^{-1} (s); UV-Vis (acetonitrile): λ_{max} (ε) = 339 (12,150), 297 (9,500), 241 nm (24,200); HRMS (ESI) *m/z*: $[M + Na]^+$ calcd. for $C_{13}H_{15}NO_6Na$, 304.0797; found, 304.0795. Anal. calcd. for $C_{13}H_{15}NO_6$: C 55.51, H 5.38, N 4.98; found: C 55.49, H 5.47, N 4.89.

Synthesis of poly[*N*-(2-hydroxypropyl)methacrylamide] (PHPMA)

HPMA (1.5 g, 10.5 mmol) and 2′,2′-azobis[2-(2-imidazolin-2-yl)propane]dihydrochloride (AIPD, 1.5 mg, 4.6 μmol) were added to a 20 mL light-shielding glass ampule. Milli-Q water (5 mL) was added to dissolve the mixture. After three freeze-pump-thaw cycles in a nitrogen atmosphere, the glass ampule was sealed and placed in a water bath at 40 °C for 48 h. At the end of polymerization, the reaction solution was diluted with Milli-Q water and added dropwise to cold acetone (400 mL) to precipitate PHPMA. This purification procedure was repeated three times, and the collected sample was dried under vacuum for 48 h at 70 °C, yielding a white solid (1.24 g, 82.7%).

GPC [DMF containing 100 mM LiBr, PS std.]: M_n = 461,000 g mol^{-1}; $M_w/M_n = 4.17$. ^{1}H NMR [500 MHz, DMSO-d_6, $\delta = 0$ ppm (TMS)]: 7.20 (br, 1H, –NH–), 4.72 (br, 1H; –OH), 3.67 (br, 1H; –CH–), 2.89 (br, 2H, –CH_2–), 1.59 (br, 2H, –CH_2–), 1.02 (br, 3H; –CH–CH_3), 0.81 (br, 3H; –C–CH_3).

Synthesis of photo-responsive block copolymers (PHPMA-*b*-PDNMA) via mechanochemical solid-state copolymerization

The block copolymers were synthesized by mechanochemical solid-state copolymerization of PHPMA and DMNBMA. Typically, the mixture of PHPMA (66.7 mg, 80 mol% as HPMA) and DMNBMA (33.3 mg, 20 mol%) was mechanically fractured in a nitrogen atmosphere with the use of a Type MM 200 mill (Retsch Co. Ltd) equipped with an agate twin-shell blender (14 mmΦ, 65 mm long) and an agate ball (6.0 mmΦ, 190 mg); additionally, the above procedure was conducted at room temperature for a prescribed period of time at 30 Hz. Residual oxygen was removed using a Model 1000 oxygen trap (Chromatography Research Supplies, Inc.) and the oxygen concentration was monitored with an oxygen analyzer (LC750/PC-120, Toray Engineering Co., Ltd) to keep the concentration below 0.01 ppm. All sample manipulations were performed in a vacuum glove box (Sanplatec Corp.), and the experiment was performed in duplicate.

Preparation of the unloaded and 5-fluorouracil (5-FU)-loaded PHPMA-*b*-PDNMA micelles

Prior to the preparation of PHPMA-*b*-PDNMA micelles, the resulting sample after 10 h of copolymerization was centrifuged (4000 rpm, 15 min × 2 cycle) with distilled water and acetone, respectively, and the precipitates after centrifugation were dried under vacuum at 60 °C for 24 h. The unloaded PHPMA-*b*-PDNMA micelles were prepared by a dialysis method. The purified PHPMA-*b*-PDNMA (20 mg) dissolved in DMF (5 mL) was placed into a dialysis bag (Spectra/Por® 3, Spectrum Laboratories, MWCO, 3500). The solution was subsequently dialyzed against phosphate-buffered saline (PBS, 0.1 M, 300 mL, pH 7.4) at room temperature for 48 h. The outer layer was exchanged at 2, 4, 6, 12, 24, and 48 h.

The 5-FU-loaded PHPMA-*b*-PDNMA micelles were also prepared through dialysis in a similar manner to that of the unloaded micelles. Briefly, purified PHPMA-*b*-PDNMA (20 mg) and 5-FU (2, 5, 10, and 20 mg) were dissolved in 5 mL of DMF and placed into a dialysis bag. The solution was dialyzed against PBS (pH 7.4) at ambient temperature for 48 h under dark conditions. The outer layer was exchanged at set intervals (2, 4, 6, 12, 24, and 48 h), and free 5-FU in the dialysate at 48 h was not observed by UV-Vis spectroscopy. In addition, both unloaded and 5-FU-loaded PHPMA-*b*-PDNMA micelles were passed through a 0.80 μm filter (GL Chromatodisc 13N, GL Sciences, Inc).

Characterization of the unloaded and 5-FU-loaded PHPMA-*b*-PDNMA micelles

To determine the 5-FU loading content (DLC) and loading efficiency (DLE) of the PHPMA-*b*-PDNMA micelles, aliquots (5 mL) of dialysate were removed at set intervals (2, 4, 6, 12, 24, and 48 h) to estimate the amount of 5-FU trapped in the micelles. The 5-FU concentration was determined by UV-Vis absorbance measurements at 266 nm. The 5-FU content of the resulting polymer micelles was calculated from a calibration curve of free 5-FU (Fig. S1). The DLC and DLE were calculated according to the following equations:

$$\mathrm{DLC}(\%) = \frac{\text{Weight of 5-FU in the micelles}}{\text{Weight of 5-FU-loaded PHPMA-}b\text{-PDNMA micelles}} \times 100\% \quad (1)$$

$$\mathrm{DLE}(\%) = \frac{\text{Weight of 5-FU in the micelles}}{\text{Weight of 5-FU in feed}} \times 100\% \quad (2)$$

The particle diameter of the unloaded and 5-FU-loaded PHPMA-*b*-PDNMA micelles was measured by DLS using a DLS-5000D Photal DLS spectrophotometer (Otsuka Electronics Co., Ltd) equipped with a He/Ne laser at 633 nm and operated at 25 °C. A scattering angle of 90° was used in this study. The particle diameter and the polydispersity were calculated using the Stokes-Einstein equation and the cumulant method, where μ_2 is the second cumulant of the decay function and Γ is the average characteristic line width [49–52]. The number-average particle diameter and weight-average particle diameter were determined by the histogram method based on the Marquardt calculation. A stability test with DLS was conducted by incubating the micelles in PBS (pH 7.4) at 37 °C for 7 days.

The morphology of the PHPMA-*b*-PDNMA micelles was examined with TEM. The negatively stained samples were measured with an H-7000 instrument (Hitachi, Ltd) operated at 125 kV at Gifu University, Gifu, Japan. For negative staining, a 200-mesh copper grid (NEM, Nisshin EM Co., Ltd) with a carbon support film (15-20 nm in thickness) was used. The copper grid was placed into the aqueous micelle solution (4 mg mL^{-1}) for 10 min at room temperature and then in distilled water for 10 s. The micelles on the grid were negatively stained three times by a 1.0% (w/v) phosphotungstic acid aqueous solution. Any excess solution was removed with filter paper. The stained sample was vacuum dried before examination.

To elucidate the photo-responsiveness of the unloaded and 5-FU-loaded PHPMA-*b*-PDNMA micelles, we measured progressive changes in the average particle diameter of the polymer micelles exposed to UV light. Typically, the unloaded and 5-FU-loaded PHPMA-*b*-PDNMA aqueous micelle solutions (4 mg mL^{-1}) were placed at a distance of 5 cm from the light source (ASONE Handy UV Lamp, SLUV-4). The aqueous solution was then exposed to UV light ($\lambda = 365$ nm) in 0.5 h intervals at room temperature, and the average particle diameter of each type of polymer micelle at those times was determined by DLS. Then, the 5-FU-loaded PHPMA-*b*-PDNMA aqueous micelle solution (4 mg mL^{-1}) that was pre-irradiated at 365 nm was transferred into dialysis membrane tubing (Spectra/Por® 3, MWCO, 3500). The tube was immersed in PBS (300 mL, pH 7.4) and stirred at ambient temperature, the external buffer of the tubing (5 mL) was collected at predetermined time intervals (0.5 and 1 h) and replaced with fresh PBS (5 mL). The concentration of 5-FU was quantified by UV analyses of the aliquots at 266 nm. 5-FU from the polymer micelles was detected by UV-Vis spectroscopy after 1 h.

Results and discussion

Synthesis and characterization of the photo-responsive block copolymer (PHPMA-*b*-PDNMA) via mechanochemical solid-state copolymerization

We performed mechanochemical solid-state copolymerization of PHPMA (number-average molecular weight (M_n) of 461,000 g mol^{-1} and polydispersity (M_w/M_n) of 4.17) and DMNBMA using an agate vessel and an agate ball at 30 Hz in a nitrogen atmosphere. Figure S2 shows the progressive changes in the ^{1}H NMR spectra of the fractured samples obtained by the mechanochemical solid-state copolymerization of PHPMA and DMNBMA, indicating that the amount of monomer (olefinic proton peak *k*) decreased over time. The polymer conversion ratio was estimated based on the rate of decrease of DMNBMA olefinic proton peaks compared with the constant signal of the added maleic acid added as an internal standard material. Figure 3 shows that the ratio of polymer conversion increased with increasing ball-milling time. We also confirmed that DMNBMA itself did not polymerize under the present experimental

conditions. Therefore, PHPMA mechanoradicals produced by the mechanolysis of PHPMA likely acted as macroinitiators for the polymerization of DMNBMA. The structures of PHPMA and PHPMA-*b*-PDNMA were confirmed from their ^{1}H NMR spectra (Figs. S3 and S4). The ratio of PHPMA and PDNMA in the block copolymer was estimated from the integrated intensity of the methylene proton signal (*d*) and that of the aromatic proton signal (*m*). The composition ratio of the hydrophilic and hydrophobic segments of the block copolymer was 2.5:1.

Figure 4 shows the progressive changes in M_n and M_w/M_n of the resulting block copolymers (PHPMA-*b*-PDNMA) and fractured PHPMA, as determined by GPC. The limit of the polymer molecular weight produced by mechanolysis depends on the frequency of ball milling and container solidity. The M_n of PHPMA-*b*-PDNMA and the fractured PHPMA decreased exponentially as the vibratory-ball milling progressed, and the M_n and M_w/M_n of PHPMA-*b*-PDNMA at 10 h were 55,800 and 2.41, respectively (Table S1). The unimodal GPC curve of PHPMA-*b*-PDNMA was clearly different from that of PHPMA as a starting material, as shown in Fig S5. At 10 h, the copolymerization of PHPMA and DMNBMA was almost complete (>90%). The PHPMA-*b*-PDNMA copolymer at 10 h was thus used for preparing the polymer micelles.

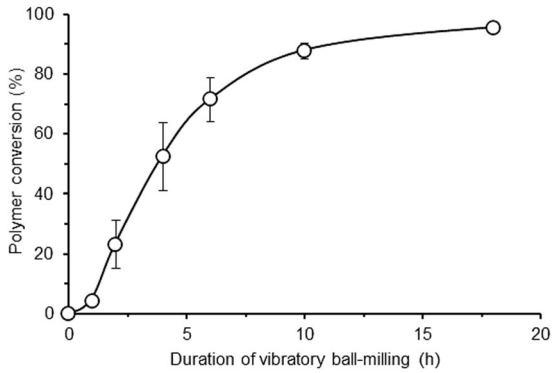

Fig. 3 Polymer conversion ratio against ball-milling time. The experiment was duplicated, and the data are expressed as the mean ± SD

Preparation and characterization of the photo-responsive unloaded PHPMA-*b*-PDNMA micelles

PHPMA-*b*-PDNMA copolymers with photolabile *o*-nitrobenzyl ester groups in PDNMA segments have the potential to form photo-responsive polymer micelles. We predicted that the PHPMA-*b*-PDNMA micelles could be disrupted by UV-light irradiation at a particular wavelength, which would indicate the photolysis of the *o*-nitrobenzyl ester groups due to the hydrophobic PDNMA segments changing to hydrophilic polymethacrylic acid. Prior to the preparation of the PHPMA-*b*-PDNMA micelles, the resulting PHPMA-*b*-PDNMA copolymer after 10 h of copolymerization was purified by the extraction of PHPMA fragments that were produced by the main-chain scission of the copolymers and residual monomers. The unloaded PHPMA-*b*-PDNMA micelles were prepared by a dialysis method in PBS (pH 7.4). The average particle diameter of the unloaded PHPMA-*b*-PDNMA micelles was 132 nm, as determined by DLS (Fig. 5). In DLS measurements, the relaxation rate Γ is proportional to the square of the scattering vector (q) and the diffusion coefficient (D), thereby leading to the following equation:

$$\Gamma = q^2 D \tag{3}$$

$$q = \frac{4\pi n_0}{\lambda_0} \sin\left(\frac{\theta}{2}\right) \tag{4}$$

where n_0 indicates the refractive index of the liquid medium, and λ_0 denotes the wavelength of the laser [53]. Spherical nanoparticles showed constant values of q over all laser angles (θ); thus, the diffusion coefficient D of the spherical nanoparticles also maintained similar values as the angle changed. Figure 6 suggests that the PHPMA-*b*-PDNMA

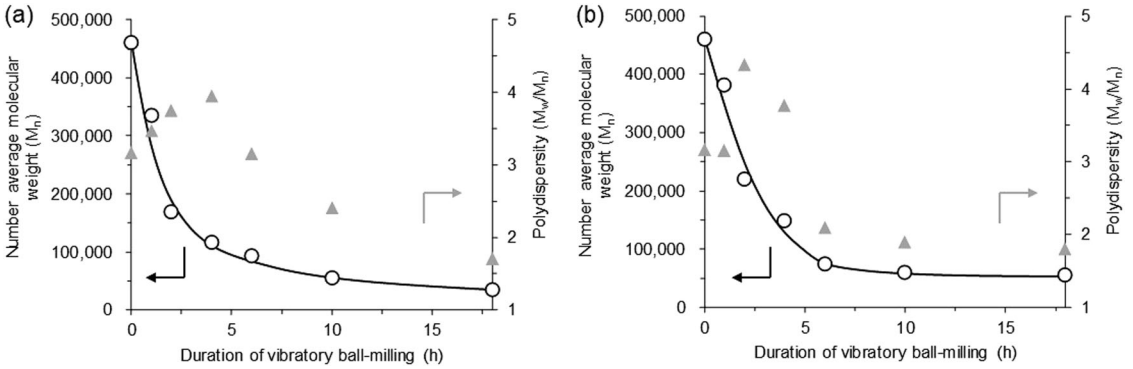

Fig. 4 Progressive changes in the number-average molecular weight (M_n) and heterogeneity (M_w/M_n) of (**a**) PHPMA and DMNBMA in the course of mechanochemical solid-state copolymerization and (**b**) fractured PHPMA, as determined by GPC in DMF containing 100 mM LiBr

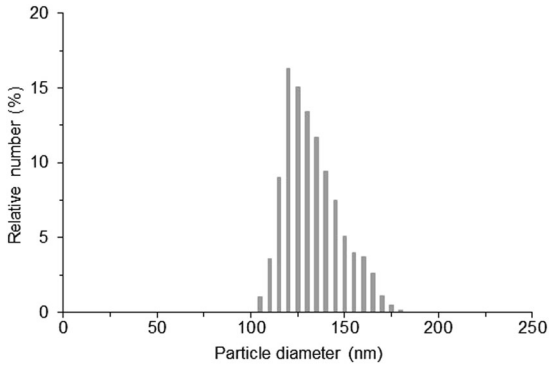

Fig. 5 Particle diameter distribution of the unloaded PHPMA-*b*-PDNMA micelles, as determined by DLS in 100 mM PBS (pH 7.4)

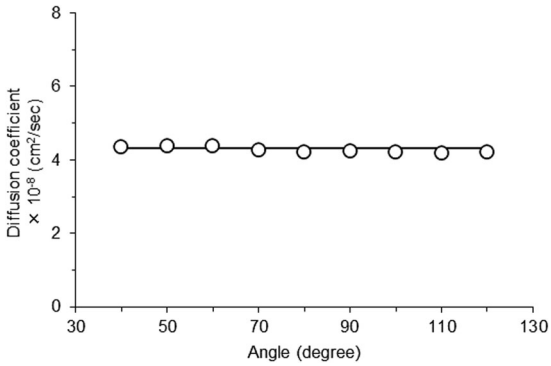

Fig. 6 Angle-dependent diffusion coefficient of the unloaded PHPMA-*b*-PDNMA micelles, as determined by DLS in 100 mM PBS (pH 7.4)

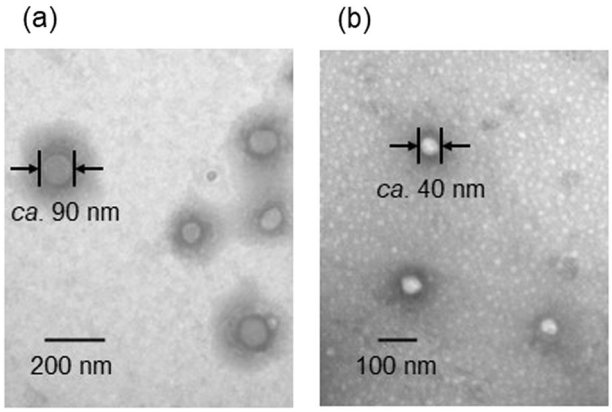

Fig. 7 TEM image of the unloaded PHPMA-*b*-PDNMA micelles negatively stained by a 1.0% (w/v) phosphotungstic acid aqueous solution **(a)** before and **(b)** after the photo irradiation at 365 nm

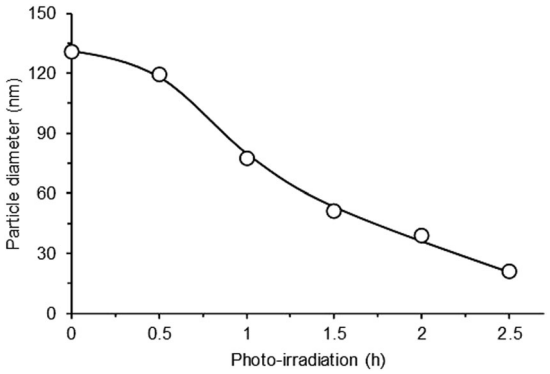

Fig. 8 Progressive changes in the average particle diameter of the unloaded PHPMA-*b*-PDNMA micelles via photo irradiation, as determined by DLS in 100 mM PBS (pH 7.4)

micelles may almost be spherical in structure, because each diffusion coefficient of the resulting micelle remained constant. TEM images obviously supported the core-shell structure of the PHPMA-*b*-PDNMA micelles (Fig. 7a). Sufficient contrast was obtained between the core and shell structure of the PHPMA-*b*-PDNMA micelles due to the negative staining of the micellar shell by phosphotungstic acid. The core size of the PHPMA-*b*-PDNMA micelles was ~50-90 nm, as shown in Fig. 7a.

The average particle diameter of the PHPMA-*b*-PDNMA micelles, as determined by DLS, also did not change when stored in PBS (pH 7.4) for 1 week at room temperature; thus, the PHPMA-*b*-PDNMA micelles were stable in aqueous solution over this time. Moreover, we investigated the photo-responsiveness of the PHPMA-*b*-PDNMA micelles under UV-light irradiation by time-course DLS measurements. UV-light ($\lambda = 365$ nm) irradiation in 0.5 h intervals was conducted against the unloaded 132 nm micelles of PHPMA-*b*-PDNMA. The average particle diameter of the PHPMA-*b*-PDNMA micelles progressively changed under UV-light exposure, as shown in Fig. 8. The DLS measurements confirmed that the average particle diameters of the PHPMA-*b*-PDNMA micelles decreased moderately with increasing UV-light ($\lambda = 365$ nm) irradiation time and were consequently below the detection limit of DLS after 3 h. Thus, the polymer micelles completely collapsed after 3 h of UV-light exposure. These results suggested that a certain UV-light irradiation time was required to dissociate the photo-responsive PHPMA-*b*-PDNMA micelles. The average particle diameter of the PHPMA-*b*-PDNMA micelles exposed to UV-light for 2 h decreased; however, the micellar core-shell structure was maintained, as shown in Fig. 7b. It can be seen in Fig. 7 that photo irradiated 40 nm micellar core was obviously smaller than the 90 nm core size before photo irradiation, because a portion of PDNMA segments that were close to PHPMA segments changed to water-soluble polymethacrylic acid moieties through photolysis.

Characterization of the 5-FU-loaded PHPMA-*b*-PDNMA micelle and its drug release via UV-light irradiation

5-FU-loaded PHPMA-*b*-PDNMA micelles were prepared in a similar manner to that of the unloaded PHPMA-*b*-PDNMA micelles. The average particle diameter of the 5-FU-loaded

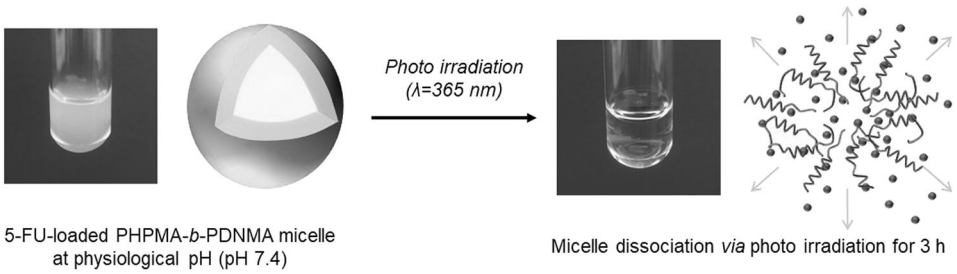

Fig. 9 Photographic images and schematic illustrations of the 5-FU-loaded PHPMA-*b*-PDNMA micelles and micellar dissociation via photo irradiation

PHPMA-*b*-PDNMA micelles (208 nm) was larger than that of the unloaded micelles owing to the encapsulation of 5-FU into the hydrophobic inner core. The DLC and DLE of the 5-FU-loaded PHPMA-*b*-PDNMA micelles were calculated to be 17.4% and 42.2%, respectively, at a free 5-FU/PHPMA-*b*-PDNMA feed ratio of 10/20 mg (Table S2). The photo irradiation-dependent 5-FU release from the PHPMA-*b*-PDNMA micelles, in which 4.2 mg of 5-FU was incorporated, was also investigated in a similar manner to that of the unloaded PHPMA-*b*-PDNMA micelles. The absorbance of 5-FU ($\lambda = 365$ nm) released from the polymer micelles was distinguished from the resulting 4,5-dimethoxy-2-nitrosobenzaldehyde by photolysis of the *o*-nitrobenzyl ester group of the PDNMA segments (Fig. S6).

Images of the 5-FU-loaded PHPMA-*b*-PDNMA micelles and the micellar dissociation are shown in Fig. 9. These clear differences indicated that the photo-responsive PHPMA-*b*-PDNMA micelles were degraded by photo irradiation. The progressive changes in the average particle diameter of the 5-FU-loaded PHPMA-*b*-PDNMA micelles exposed to UV-light are shown in Fig. 10 (shown as a solid line). Figure 10 shows that an initial lag time was observed. It was considered that the photolysis of the *o*-nitrobenzyl ester groups might slowly progress to impede the penetration of water molecules into the hydrophobic micellar core. We also revealed that the profile showing the decrease in micellar size followed a sigmoid function and that the corresponding curve fitting was determined by logistic regression (shown as the dotted line in Fig. 10). The photo irradiation induced time-dependent changes in the particle diameter of the unloaded and 5-FU-loaded PHPMA-*b*-PDNMA micelles depicted in Figs. S7 and 10 fit the equations as follows:

$$\text{Size reduction kinetics of unloaded micelles (nm)} = \frac{176.042}{(1 + 0.312e^{1.295x})} \quad (5)$$

$$\text{Size reduction kinetics of drug-loaded micelles (nm)} = \frac{280.024}{(1 + 0.306e^{1.270x})} \quad (6)$$

where the numerator indicates the upper limits of micellar size, and the exponents of *e* denote the initial slope of the

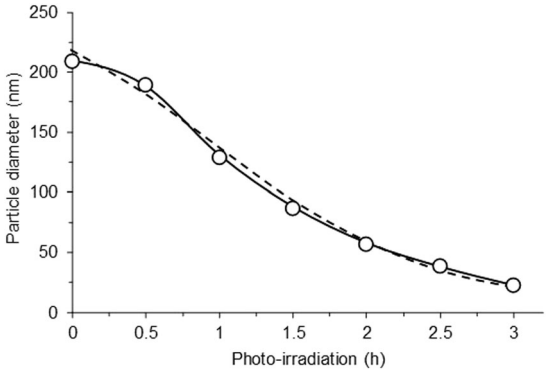

Fig. 10 Progressive changes in the average particle diameter (solid line) and curve fitting (dotted line) of the 5-FU-loaded PHPMA-*b*-PDNMA micelles

logistic model. Although the upper limits were appreciably different between the unloaded and drug-loaded micelles, the slopes of each equation were in good agreement. Therefore, it was considered that the collapse behavior of the PHPMA-*b*-PDNMA micelles might be similar to each other, regardless of whether drugs were incorporated in the micellar core. These findings suggested that the photolysis of the hydrophobic regions with H_2O might be the rate-determining step.

Figure 11 shows that the progressive changes in the drug release from the 5-FU-loaded PHPMA-*b*-PDNMA micelles exposed to UV-light completely followed a sigmoidal model (shown as the solid line), similar to that of the decrease in micellar size. The photo irradiation induced time-dependent changes in the 5-FU release from the PHPMA-*b*-PDNMA micelles depicted in Fig. 11 were in good agreement with the curve fitting results of the following equation:

$$\text{5-FU release rate from polymer micelles (\%)} = \frac{92.469}{(1 + 49.572e^{-3.220x})} \quad (7)$$

Notably, the released 5-FU profile of the 5-FU-loaded PHPMA-*b*-PDNMA micelles depended on the photo irradiation time, as shown in Fig. 12. After the release of a

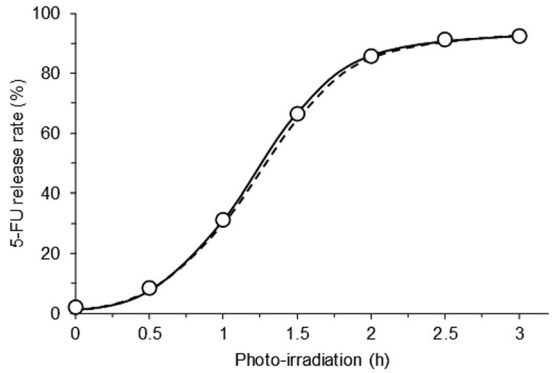

Fig. 11 Progressive changes in the drug release (solid line) and curve fitting (dotted line) of the 5-FU-loaded PHPMA-*b*-PDNMA micelles

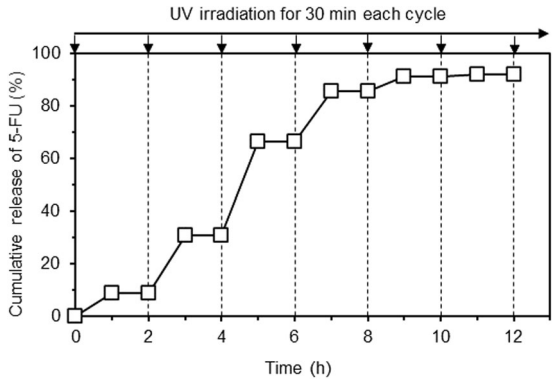

Fig. 12 Cumulative drug release from the 5-FU-loaded PHPMA-*b*-PDNMA micelles via photo irradiation for each 30 min cycle

certain quantity of 5-FU from the 5-FU-loaded PHPMA-*b*-PDNMA micelles exposed to UV-light, a sustained 5-FU release and a decrease in the average particle diameter did not occur spontaneously. Therefore, the PHPMA-*b*-PDNMA micelles released the required amount of loaded drugs via photo irradiation, thus demonstrating its potential for use as an on-demand controlled drug release system.

Conclusions

This study focused on photo-responsive polymer micelles from amphiphilic block copolymers (PHPMA-*b*-PDNMA) synthesized by mechanochemical solid-state copolymerization for use in applications of controlled drug release. The mechanochemical solid-state copolymerization of PHPMA and DMNBMA, which had photosensitive *o*-nitrobenzyl ester groups, proceeded almost quantitatively after 10 h, thus producing PHPMA-*b*-PDNMA with an M_n of 26,500 and an M_w/M_n of 1.39 after purification. The average particle diameters of the unloaded PHPMA-*b*-PDNMA micelles and 5-FU-loaded PHPMA-*b*-PDNMA micelles were 132 and 208 nm, respectively. The 5-FU-loaded PHPMA-*b*-PDNMA micelles were also stable in pH 7.4 and dissociated under UV irradiation to release 5-FU. The decrease in micellar size and drug release kinetics via photo irradiation clearly followed a sigmoid curve, and their profiles were represented by well-defined formulas. The 5-FU-loaded PHPMA-*b*-PDNMA micelles showed a quantitative drug release after a certain period of photo irradiation. These results suggest that photo-responsive PHPMA-*b*-PDNMA micelles are effective anticancer drug carriers that can be used for an on-demand controlled drug release.

Acknowledgements This work was supported by a grant from the OGAWA Science and Technology Foundation. We also give thanks to Springer Nature Author Services for editing a draft of this manuscript.

Compliance with ethical standards

Conflict of interest The authors declare that they have no conflict of interest.

Publisher's note Springer Nature remains neutral with regard to jurisdictional claims in published maps and institutional affiliations.

References

1. Li KC, Pandit SD, Guccione S, Bednarski MD. Molecular imaging applications in nanomedicine. Biomed Microdevices. 2004;6:113–6.
2. Moghimi SM, Hunter AC, Murray JC. Nanomedicine: current status and future prospects. FASEB J. 2005;19:311–30.
3. Nasongkla N, Bey E, Ren J, Ai H, Khemtong C, Guthi JS, et al. Multifunctional polymeric micelles as cancer-targeted, MRI-ultrasensitive drug delivery systems. Nano Lett. 2006;6:2427–30.
4. Skinner SA, Tutton PJM, O'Brien PE. Microvascular architecture of experimental colon tumors in the rat. Cancer Res. 1990;50:2411–7.
5. Suzuki M, Hori K, Abe I, Saito S, Sato H. A new approach to cancer chemotherapy: selective enhancement of tumor blood flow with angiotensin II. J Natl Cancer Inst. 1981;67:663–9.
6. Maeda H, Matsumura Y. Tumoritropic and lymphotropic principles of macromolecular drugs. Crit Rev Ther Drug Carr Syst. 1989;6:193–210.
7. Iwai K, Maeda H, Konno T. Use of oily contrast medium for selective drug targeting to tumor: enhanced therapeutic effect and X-ray image. Cancer Res. 1984;44:2115–21.
8. Matsumura Y, Maeda H. A new concept for macromolecular therapeutics in cancer chemotherapy: mechanism of tumoritropic accumulation of proteins and the antitumor agent smancs. Cancer Res. 1986;46:6387–92.
9. Cammasa S, Suzuki K, Sone C, Sakurai Y, Kataoka K, Okano T. Thermo-responsive polymer nanoparticles with a core-shell micelle structure as site-specific drug carriers. J Controlled Release. 1997;48:157–64.
10. Chung JE, Yokoyama M, Okano T. Inner core segment design for drug delivery control of thermo-responsive polymeric micelles. J Controlled Release. 2000;65:93–103.
11. Liang X, Liu F, Kozlovskaya V, Palchak Z, Kharlampieva E. Thermoresponsive micelles from double LCST-Poly(3-methyl-N-vinylcaprolactam) block copolymers for cancer therapy. ACS Macro Lett. 2015;4:308–11.

12. Hassanzadeh F, Farzan M, Varshosaz J, Khodarahmi GA, Maaleki S, Rostami M. Poly (ethylene-co-vinyl alcohol)-based polymeric thermo-responsive nanocarriers for controlled delivery of epirubicin to hepatocellular carcinoma. Res Pharm Sci. 2017;12:107–18.
13. Zhao Y. Photocontrollable block copolymer micelles: what can we control? J Mater Chem. 2009;19:4887–95.
14. Ercole F, Davis TP, Evans RA. Photo-responsive systems and biomaterials: photochromic polymers, light-triggered self-assembly, surface modification, fluorescence modulation and beyond. Polym Chem. 2010;1:37–54.
15. Schumers JM, Fustinand CA, Gohy JF. Light-responsive block copolymers. Macromol Rapid Commun. 2010;31:1588–607.
16. Pasparakis G, Manouras T, Argitis P, Vamvakaki M. Photodegradable polymers for biotechnological applications. Macromol Rapid Commun. 2012;33:183–98.
17. Zhao Y. Light-responsive block copolymer micelles. Macromolecules. 2012;45:3647–57.
18. Husseini GA, Myrup GD, Pitt WG, Christensen DA, Rapoport NY. Factors affecting acoustically triggered release of drugs from polymeric micelles. J Control Release. 2000;69:43–52.
19. Gao Z, Fain HD, Rapoport N. Ultrasound-enhanced tumor targeting of polymeric micellar drug carriers. Mol Pharm. 2004; 1:317–30.
20. Zhang H, Xia H, Wang J, Li Y. High intensity focused ultrasound-responsive release behavior of PLA-b-PEG copolymer micelles. J Control Release. 2009;139:31–9.
21. Wu P, Jia Y, Qu F, Sun Y, Wang P, Zhang K, et al. Ultrasound-responsive polymeric micelles for sonoporation-assisted site-specific therapeutic action. ACS Appl Mater Interfaces. 2017;9: 25706–16.
22. Bae Y, Nishiyama N, Fukushima S, Koyama H, Matsumura Y, Kataoka K. Preparation and biological characterization of polymeric micelle drug carriers with intracellular pH-triggered drug release property: tumor permeability, controlled subcellular drug distribution, and enhanced in vivo antitumor efficacy. Bioconjugate Chem. 2005;16:122–30.
23. Convertine AJ, Diab C, Prieve M, Paschal A, Hoffman AS, Johnson PH, et al. pH-responsive polymeric micelle carriers for siRNA drugs. Biomacromolecules. 2010;11:2904–11.
24. Kondo S, Yamamoto K, Sawama Y, Sasai Y, Yamauchi Y, Kuzuya M. Characterization of novel pH-sensitive polymeric micelles prepared by the self-assembly of amphiphilic block copolymer with poly-4-vinylpyridine block synthesized by mechanochemical solid-state polymerization. Chem Pharm Bull. 2011;59:1200–2.
25. Kondo S, Asano Y, Koizumi N, Tatematsu K, Sawama Y, Sasai Y, et al. Novel pH-responsive polymeric micelles prepared through self-assembly of amphiphilic block copolymer with poly-4-vinylpyridine block synthesized by mechanochemical solid-state polymerization. Chem Pharm Bull. 2015;63:489–94.
26. Hiruta Y, Kanda Y, Katsuyama N, Kanazawa H. Dual temperature- and pH-responsive polymeric micelle for selective and efficient two-step doxorubicin delivery. RSC Adv. 2017;7: 29540–49.
27. Li Q, Yao W, Yu X, Zhang B, Dong J, Jin Y. Drug-loaded pH-responsive polymeric micelles: simulations and experiments of micelle formation, drug loading and drug release. Colloids Surf B Biointerfaces. 2017;158:709–16.
28. Zhao H, Sterner ES, Coughlin EB, Theato P. *o*-nitrobenzyl alcohol derivatives: opportunities in polymer and materials science. Macromolecules. 2012;45:1723–36.
29. Zhao Y. Rational design of light-controllable polymer micelles. Chem Rec. 2007;7:286–94.
30. Gohy J-F, Zhao Y. Photo-responsive block copolymer micelles: design and behavior. Chem Soc Rev. 2013;42:7117–29.
31. Abreu CMR, Mendonça PV, Serra AC, Coelho JFJ, Popov AV, Guliashvili T. Accelerated ambient-temperature ATRP of methyl acrylate in alcohol-water solutions with a mixed transition-metal catalyst system. Macromol Chem Phys. 2012;213:1677–87.
32. Ding M, Jiang X, Zhang L, Cheng Z, Zhu X. Recent progress on transition metal catalyst separation and recycling in ATRP. Macromol Rapid Commun. 2015;36:1702–21.
33. Frazer L. Radical departure: polymerization does more with less. Environ Health Perspect. 2007;115:A258–61.
34. Kuzuya M, Kondo S, Noguchi A. A new development of mechanochemical solid-state polymerization of vinyl monomers: prodrug syntheses and its detailed mechanistic study. Macromolecules. 1991;24:4047–53.
35. Kuzuya M, Kondo S, Noguchi A, Noda N. Mechanistic study on mechanochemical polymerization of acrylamide. J Polym Sci Part A Polym Chem. 1991;29:489–94.
36. Kuzuya M, Kondo S, Noguchi A, Noda N. Nature of mechanoradical formation and reactivity with oxygen in methacrylic vinyl polymers. J Polym Sci Part B Polym Phys. 1992;30:97–103.
37. Kondo S, Sasai Y, Hosaka S, Ishikawa T, Kuzuya M. Kinetic analysis of the mechanolysis of polymethylmethacrylate in the course of vibratory ball milling at various mechanical energy. J Polym Sci Part A Polym Chem. 2004;42:4161–67.
38. Kuzuya M, Yamauchi Y, Kondo S. Mechanolysis of glucose-based polysaccharides as studied by electron spin resonance. J Phys Chem B. 1999;103:8051–9.
39. Sasai Y, Yamauchi Y, Kondo S, Kuzuya M. Nature of mechanoradical formation of substituted celluloses as studied by electron spin resonance. Chem Pharm Bull. 2004;52:339–44.
40. Doi N, Sasai Y, Yamauchi Y, Adachi T, Kuzuya M, Kondo S. Kinetic analysis of mechanoradical formation during the mechanolysis of dextran and glycogen. Beilstein J Org Chem. 2017;13:1174–83.
41. Kondo S, Hatakeyama I, Hosaka S, Kuzuya M. Mechanochemical solid-state polymerization (X): the influence of copolymer structure in copolymeric prodrugs on the nature of drug release. Chem Pharm Bull. 2000;48:1882–5.
42. Kondo S, Mori H, Sasai Y, Kuzuya M. Conventional synthesis of amphiphilic block copolymer utilized for polymeric micelle by mechanochemical solid-state polymerization. Chem Pharm Bull. 2007;55:389–92.
43. Doi N, Sasai Y, Yamauchi Y, Adachi T, Kuzuya M, Kondo S. Development of novel polymeric prodrugs synthesized by mechanochemical solid-state copolymerization of hydroxyethylcellulose and vinyl monomers. Chem Pharm Bull. 2015;63:992–7.
44. Doi N, Sasai Y, Yamauchi Y, Adachi T, Kuzuya M, Kondo S. A novel polymeric prodrugs synthesized by mechanochemical solid-state copolymerization of glucose-based polysaccharides and vinyl monomers. Int J Pharm Sci Invent. 2017;6:38–46.
45. Duncan R. The drawing era of polymer therapeutics. Nat Rev Drug Discov. 2003;2:347–60.
46. Kopeček J, Kopečková P, Minko T, Lu Z. HPMA copolymer-anticancer drug conjugates: design, activity, and mechanism of action. Eur J Pharm Biopharm. 2000;50:61–81.
47. Říhová B, Kubáčková K. Clinical implications of N-(2-hydroxypropyl)methacrylamide copolymers. Curr Pharm Biotechnol. 2003;4:311–22.
48. Talelli M, Rijcken CJF, van Nostrum CF, Storm G, Hennink WE. Micelles based on HPMA copolymers. Adv Drug Deliv Rev. 2010;62:231–9.
49. Kim K, Kwon S, Park JH, Chung H, Jeong SY, Kwon IC, et al. Physicochemical characterizations of self-assembled nanoparticles of glycol chitosan-deoxycholic acid conjugates. Biomacromolecules. 2005;6:1154–8.
50. Nam HY, Kwon SM, Chung H, Lee SY, Kwon SH, Jeon H, et al. Cellular uptake mechanism and intracellular fate of hydrophobically

modified glycol chitosan nanoparticles. J Control Release. 2009; 135:259–67.
51. Stankovich S, Piner RD, Nguyen S-BT, Ruoff RS. Synthesis and exfoliation of isocyanate-treated graphene oxide nanoplatelets. Carbon. 2006;44:3342–47.
52. Park C, Lee IH, Lee S, Song Y, Rhue M, Kim C. Cyclodextrin-covered organic nanotubes derived from self-assembly of dendrons and their supramolecular transformation. Proc Natl Acad Sci USA. 2006;103:1199–203.
53. Li X, Mya KY, Ni X, He C, Leong KW, Li J. Dynamic and static light scattering studies on self-aggregation behavior of biodegradable amphiphilic poly(ethylene oxide)-poly[(R)-3-hydroxybutyrate]-poly(ethylene oxide) triblock copolymers in aqueous solution. J Phys Chem B. 2006;110:5920–6.